

# Highly Flexible $\pi$ -Expanded Cyclooctatetraenes: Cyclic Thiazole Tetramers with Head-to-Tail Connection\*\*

Kazuhiro Mouri, Shohei Saito, and Shigehiro Yamaguchi\*

Flexible  $\pi$ -conjugated skeletons have been the focus of considerable interest because their dynamic molecular motions can be the basis of interesting molecule-based functions. Representative examples of dynamic  $\pi$  systems include the corannulenes<sup>[1]</sup> and the sumanenes,<sup>[2]</sup> which exhibit a bowl-to-bowl inversion behavior, helicene derivatives that undergo flipping,<sup>[3]</sup> twisted bay-substituted perylene bisimides,<sup>[4]</sup> and expanded porphyrins<sup>[5]</sup> of various topologies. Cyclooctatetraene (COT), an  $8\pi$  annulene, is one of the classical flexible  $\pi$ -conjugated skeletons that has long been studied from both theoretical and experimental points of view.<sup>[6]</sup> The instability of its planar conformation, is attributable to its angle strain and antiaromaticity,<sup>[7]</sup> and causes this skeleton to have a nonplanar tub structure in the ground state; notably, this structure undergoes a tub-to-tub inversion in solution (Figure 1 a).<sup>[8]</sup> Additionally, in response to reduction or oxidation, this tub-shaped skeleton can undergo a structural change into a planar form because of the aromaticity of the reduced  $10\pi$  dianion<sup>[9]</sup> or the oxidized  $6\pi$  dication.<sup>[10]</sup> Various fascinating COT materials that make use of these dynamic behaviors have been developed, and include cavity-size-controlled cage molecules,<sup>[11]</sup> electromechanical actuators,<sup>[12]</sup> buckycatchers,<sup>[13]</sup> and molecular tweezers.<sup>[14]</sup>

More sophisticated COT materials need to be thermally stable and this property can be ensured through a design that incorporates arene rings fused to the COT structure. However, this approach destabilizes the planar conformation of the COT skeleton because of the steric repulsion between neighboring fused arene rings, thereby increasing the tub-to-tub inversion barrier. A completely planar COT can be accessed by preparing a polyarene-fused structure, as reported by Nishinaga, Iyoda, and co-workers.<sup>[15]</sup> In contrast, we were interested in accessing a flexible and planarizable COT in the form of a tetraarene-fused structure, specifically a COT skeleton containing four thiazole rings arranged in a head-to-tail manner (Figure 1 b). We believed that, despite the tetraarene-fused structure of this COT skeleton, the alternating arrangement of the nitrogen and sulfur atoms, which take the place of the peripheral C–H bonds in phenyl-fused derivatives, should lead to a low level of steric repulsion, thereby enhancing the flexibility of the COT skeleton, and allow it to take a planar conformation upon reduction or oxidation. Moreover, we envisioned that the introduction of aryl groups on the 2-position of the four thiazole rings of the head-to-tail skeleton would allow for effective expansion of the  $\pi$  conjugation. Herein, we describe the synthesis of cyclic thiazole tetramers **1** and discuss their structural characteristics in comparison to those of the head-to-head isomer **2**.

The head-to-tail cyclic tetramers **1** were prepared using two different routes, each employing a Pd-catalyzed C–H arylation of thiazole rings:<sup>[16]</sup> route A) intramolecular ring closure of acyclic thiazole tetramers **6** under high-dilution conditions; route B) intermolecular double C–H arylation of thiazole dimers **4** (Scheme 1). The final ring-closing steps in both routes proceeded with acceptable yields, 62 % yield of **1a** (from **6a**; route A) and 36 % yield of **1a** (from **4a**; route B). The high efficiencies of these transformations may be attributable to the geometries of the acyclic thiazole tetramer precursors. Based on DFT calculations,<sup>[17]</sup> a U-shaped bent conformation of **5a** is more stable than its Z-shaped conformation by 8.0 kcal mol<sup>−1</sup>, and thereby the ring-closure reaction should be more favorable than polymerization (see the Supporting Information). The U-shaped conformation of **5a** was confirmed by the crystal structure (Figure 2).<sup>[18]</sup> It is also worth noting that the use of the thiazole dimers **4** is crucial for the preparation of cyclized product **1** using route B. Whereas the intermolecular C–H arylation of **4** gave the cyclized products **1**, the reaction of the regioisomers **3** did not yield **1**, presumably owing to the lower reactivity of the C–H bond at the 4-position of the thiazole toward the direct arylation. A head-to-head cyclic thiazole tetramer **2a** (Ar = *p*-Tol) was prepared by the oxidative homocoupling of a dilithiated precursor according to the

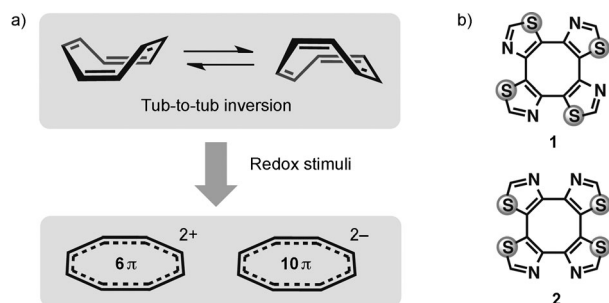
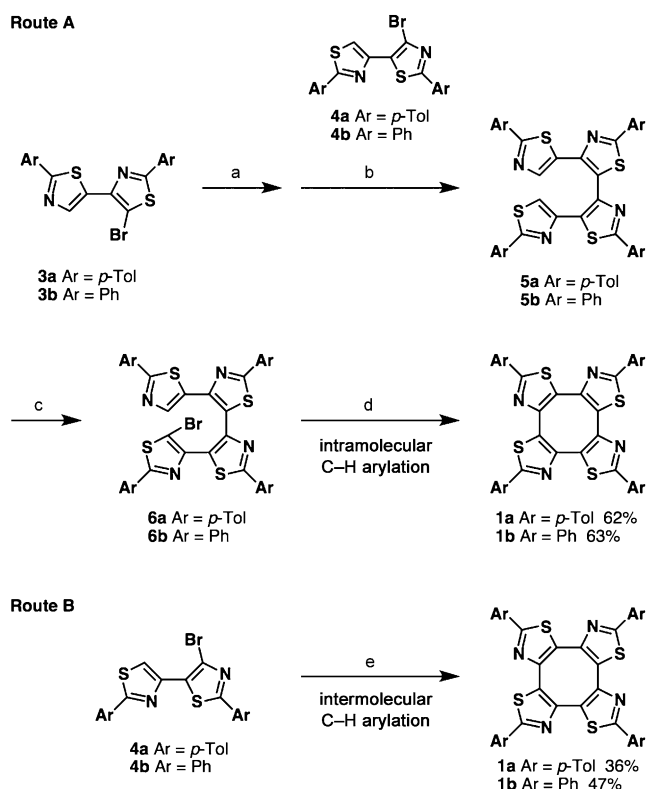


**Figure 1.** a) Dynamic conformational change of COT and b) molecular structures of head-to-tail cyclic thiazole tetramer **1** and its head-to-head isomer **2**.

[\*] K. Mouri, Dr. S. Saito, Prof. Dr. S. Yamaguchi  
Department of Chemistry, Graduate School of Science  
Nagoya University, and  
CREST, Japan Science and Technology Agency  
Furo, Chikusa, Nagoya 464-8602 (Japan)  
E-mail: yamaguchi@chem.nagoya-u.ac.jp

[\*\*] This work was supported by CREST and JST. K.M. thanks the JSPS for a Research Fellowship for Young Scientists. S.S. thanks the Noguchi Institute, Japan Association for Chemical Innovation, and The Kurata Memorial Hitachi Science and Technology Foundation for grants.

Supporting information for this article is available on the WWW under <http://dx.doi.org/10.1002/anie.201201265>.



**Scheme 1.** Synthesis of cyclic thiazole tetramers with a head-to-tail connection. Reagents and conditions a) 1. *n*BuLi, THF,  $-78^{\circ}\text{C}$ ; 2.  $\text{ZnCl}_2(\text{tmeda})$ ,  $-78^{\circ}\text{C}$  then RT; b)  $[\text{Pd}_2(\text{dba})_3]\cdot\text{CHCl}_3$ ,  $55^{\circ}\text{C}$ ; c) NBS,  $\text{CHCl}_3/\text{DMF}$ ,  $60^{\circ}\text{C}$ ; d)  $\text{Pd}(\text{OAc})_2$ , XPhos,  $\text{Cs}_2\text{CO}_3$ , *m*-xylene (0.01 M),  $140^{\circ}\text{C}$ , 4 days; e)  $\text{Pd}(\text{OAc})_2$ , PPh<sub>3</sub>, PivOH,  $\text{K}_2\text{CO}_3$ , DMA (0.25 M),  $100^{\circ}\text{C}$ , 1 day. dba = dibenzylideneacetone, DMA = *N,N'*-dimethylacetamide, DMF = *N,N'*-dimethylformamide, NBS = *N*-bromosuccinimide, Piv = pivaloyl, tmeda = *N,N,N',N'*-tetramethylethylenediamine, Tol = tolyl, XPhos = 2-dicyclohexylphosphino-2',4',6'-triisopropylbiphenyl.

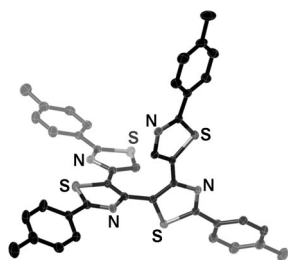


**Figure 2.** X-ray crystal structure of **5a**. Hydrogen atoms are omitted for clarity and thermal ellipsoids are shown at 50% probability.

method reported for the synthesis of a cyclic thiophene tetramer (see the Supporting Information).<sup>[19]</sup>

A thermogravimetric analysis (TGA) revealed the high thermal stability of **1a**: the decomposition temperature for a 5% weight loss ( $T_{d5}$ ) was  $421^{\circ}\text{C}$ . This high stability is attributable to its molecular structure, in which the central COT moiety is fused with aromatic thiazole rings, the reactive 2-positions of which are capped by aryl substituents. Single-crystal X-ray diffraction analysis of **1a** and **2a** revealed their saddle-shaped structures wherein the central COT moieties were in the tub conformation (Figure 3 and the Supporting

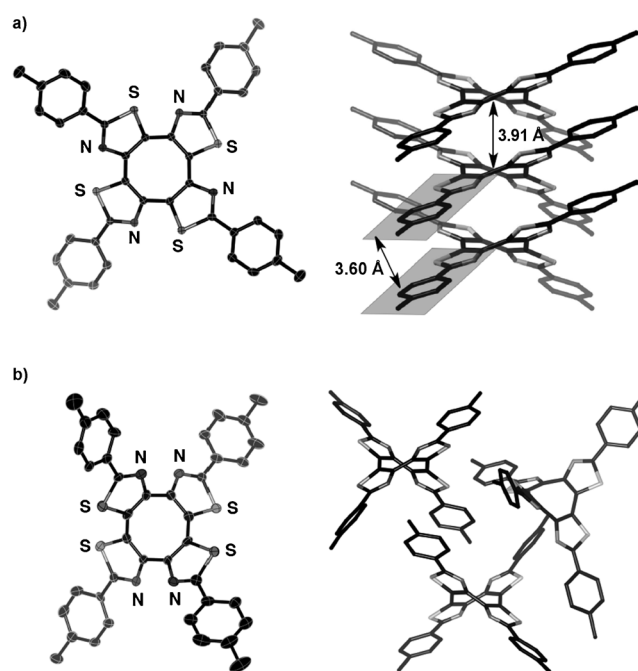
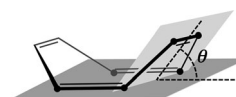


**Figure 3.** X-ray crystal structures of a) **1a** and b) **2a**. Molecular structures are shown on the left wherein thermal ellipsoids are shown at 50% probability; crystal packing is shown on the right. Hydrogen atoms are omitted for clarity.

Information).<sup>[18]</sup> In all the compounds, the thiazole rings and the aryl substituents have conformations that make them almost coplanar, which is indicative of an expanded  $\pi$  conjugation. Importantly, the tub structure of the COT moiety in the head-to-tail tetramer **1a** is shallower than that in the head-to-head isomer **2a**. The bent angle  $\theta$ <sup>[15]</sup> of the COT skeleton in **1a** is  $29^{\circ}$ , which is much smaller than that in **2a** ( $40^{\circ}$ ), and is the smallest value among those of known tetraarene-fused COT molecules ( $38\text{--}49^{\circ}$ ).<sup>[12a,20]</sup> The rela-



tively shallow tub geometry of **1a** is stabilized by the following structural features: 1) the thiazole rings, which do not experience the same repulsive interactions with their neighbors as do phenyl rings because of the absence of peripheral C–H bonds; 2) the alternating arrangement of the nitrogen and sulfur atoms in the head-to-tail tetramer skeleton. The size of the bent angles may affect the electronic characters of the COT moieties. To assess the aromaticity of these compounds, their NICS (nucleus-independent chemical shift)<sup>[21]</sup> values were examined. The NICS values at the mean coordinate of the eight-membered ring in the optimized geometries are +6.2 ppm for **1a** and +3.3 ppm for **2a** at the B3LYP/6-311 + G\*\* level of theory.<sup>[17]</sup> These results suggest that the shallow tub COT structure in **1a** slightly perturbs the antiaromatic character, although both are essentially non-aromatic compounds.<sup>[15]</sup>

In their crystal forms, both **1a** and **1b** pack together through columnar stacking, despite their nonplanar struc-

tures. In the structure of **1a**, the intermolecular distance between the mean planes of the adjacent arylthiazole units is 3.60 Å and the tub-shaped COT cores are stacked with an intermolecular distance of 3.91 Å (Figure 3a). The large contact area between the adjacent saddle-shaped molecules results in a strong van der Waals interaction, which may be responsible for the columnar stacking. In line with these structural features, **1a** and **1b** have poor solubilities in common organic solvents. In light of the fact that regioisomer **2a** does not stack in a columnar form, it seems that the head-to-tail arrangement of thiazole moieties in **1a** is crucial for realizing these stacking structures (Figure 3b).

The shallow tub structure of **1** prompted us to investigate the tub-to-tub inversion behavior of this molecular system. DFT (B3LYP/6-31G\*) calculations revealed that the tub-to-tub inversion barrier of COT **1** has the unusually low value of  $\Delta G^\ddagger = 6.8 \text{ kcal mol}^{-1}$  at 298 K.<sup>[17]</sup> This inversion should proceed along a simple bell-shaped energy profile via a planar transition state; this hypothesis was confirmed by the IRC (intrinsic reaction coordinate) calculation (Figure 4a).<sup>[22]</sup> Notably, this inversion barrier is the lowest value among those of known COT derivatives, including the nonsubstituted parent COT skeleton **8** (10.9 kcal mol<sup>-1</sup>),<sup>[8]</sup> and is even lower than the bowl-to-bowl inversion barriers of corannulene (11.5 kcal mol<sup>-1</sup>)<sup>[1b]</sup> and sumanene (18.8 kcal mol<sup>-1</sup>),<sup>[2c]</sup> and the flipping barrier of the bay-substituted perylene bisimide (14.3 kcal mol<sup>-1</sup>).<sup>[4]</sup> The value of  $\Delta G^\ddagger = 6.8 \text{ kcal mol}^{-1}$  corresponds to a frequency of  $6.4 \times 10^7 \text{ s}^{-1}$  at 298 K. Although it is difficult to experimentally confirm such a low energy barrier, for example, by means of variable temperature NMR experiments, this structural feature should render this skeleton a unique flexible  $\pi$ -conjugated system.

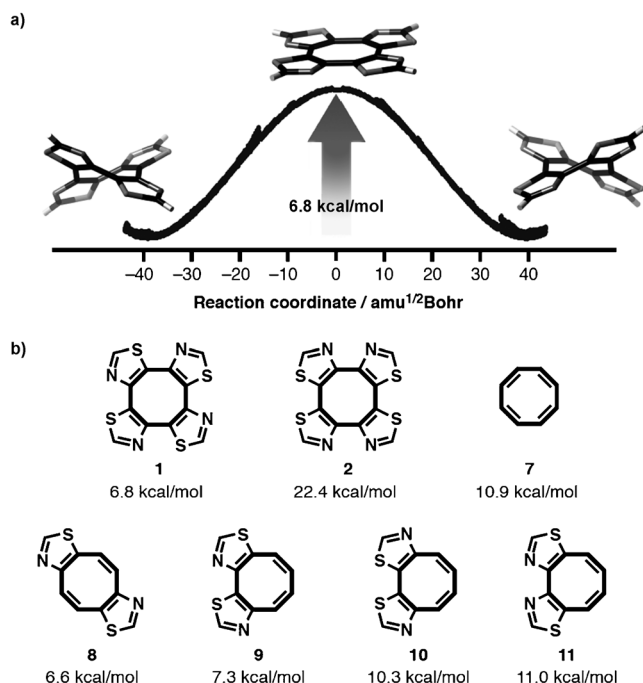


**Figure 4.** a) Relative energy diagram of the tub-to-tub inversion of **1** based on the IRC calculation and b) inversion barriers of the parent COT and thiazole-fused COT derivatives calculated at the B3LYP/6-31G\* level of theory.

We then focused on the origin of the significantly low inversion barrier of **1**. It can be rationalized by the following three considerations. Firstly, the small C=C-S angles of the thiazoles, which are fused to the COT framework, cause a rehybridization of the carbon atoms within the COT eight-membered ring; this hybridization leads to wider inner angles of the COT ring.<sup>[7]</sup> As the inner angle of a regular octagon (135°) is larger than the ideal bond angle for a  $\text{sp}^2$  hybridized carbon atom (120°), the widening of the inner angles results in a shallower tub-shaped COT structure. Accordingly, the bent angle  $\theta$  (34.5°) of **1** in the optimized structure is smaller than that of the nonsubstituted COT **7** (39.4°).<sup>[23]</sup> It is known that the annulation of ring skeletons having small inner bond angles reduces the bent angle of COT.<sup>[7c,d,i]</sup> This structural effect should also lead to reduced angle strain in the planar COT structure of the transition state, thus leading to the lower inversion barrier (Figure 4b). Secondly, the low level of steric hindrance between neighboring thiazole rings in the head-to-tail arrangement should contribute substantially to the relative stability of the planar transition-state structure of **1**. Indeed, the head-to-head regioisomer **2**, which has more significant levels of steric hindrance between neighboring thiazoles, has a far higher inversion barrier of 22.4 kcal mol<sup>-1</sup>. A comparison of the inversion barriers among a series of dithiazole-fused COT skeletons that included **8** (6.6 kcal mol<sup>-1</sup>), **9** (7.3 kcal mol<sup>-1</sup>), **10** (10.3 kcal mol<sup>-1</sup>), and **11** (11.0 kcal mol<sup>-1</sup>) clearly demonstrates that the head-to-tail arrangement engenders a lower inversion barrier. Thirdly, the presence of fused thiazole rings in **1** should mean that in the transition state, in which the COT core takes on a planar conformation, the antiaromaticity of the COT core of **1** is relatively low; this lower antiaromaticity would result in a smaller antiaromatic destabilization of the transition state for **1** than for the nonsubstituted COT **7**.<sup>[7e,g]</sup> The NICS(0) values of the tetrathiazole-fused COT **1**, dithiazole-fused COT **8**, and nonsubstituted COT **7** were estimated to be +17.2, +24.2, and +42.1 ppm, respectively, in the transition state (see the Supporting Information), thus demonstrating the significant difference in the antiaromaticity. These considerations lead to the conclusion that the head-to-tail arrangement of thiazole rings is optimal for achieving a flexible COT skeleton.

We next investigated the structural changes in the tetrathiazole-fused COT upon its reduction or oxidation. We first obtained cyclic voltammetry responses of **1a** in  $\text{CH}_2\text{Cl}_2$  or THF and compared them to those of the noncyclic congener **5a** (Figure 5). The cyclic **1a** showed reversible redox waves at the first oxidation potential of  $E_{\text{ox}} = +0.67 \text{ V}$  and at the first and second reduction potentials of  $E_{\text{red}} = -1.93 \text{ V}$  and  $-2.19 \text{ V}$  (versus  $\text{Fc}/\text{Fc}^+$ ), respectively; the noncyclic tetramer **5a** only showed irreversible processes during both oxidation and reduction with a more positive anodic peak potential of  $E_{\text{pa}} = +0.92 \text{ V}$  and a more negative first cathodic peak potential of  $E_{\text{pc}} = -2.46 \text{ V}$ . These results demonstrate that the oxidation and reduction of the thiazole tetramer  $\pi$  skeleton is facilitated when the skeleton is in the cyclic form, and that the central COT moiety endows this skeleton with high redox stability.

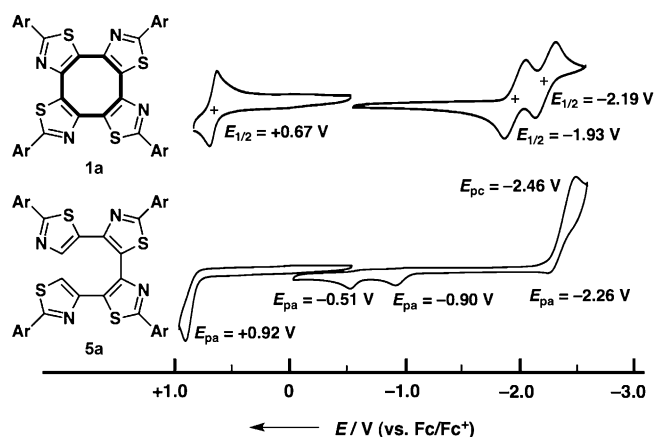


**Figure 5.** Cyclic voltammograms of **1a** and **5a** in  $\text{CH}_2\text{Cl}_2$  for oxidation and in THF for reduction. Fc = ferrocene.

Consistent with the redox stability, the chemical reduction of **1a** led to a dianion species. The addition of potassium metal to a THF suspension of **1a** resulted in a dramatic color change from light yellow to deep purple together with the obvious changes in the  $^1\text{H}$  and  $^{13}\text{C}$  NMR spectra (see the Supporting Information). Upon the addition of [2.2.2]cryptand to the solution, single crystals of the dianion salt **1a** $^{2-} \cdot 2[\text{K}(\text{cryptand})]^+$  were obtained. The X-ray crystal structure revealed that the reduced COT moiety indeed has a completely planar geometry ( $\theta = 1.5^\circ$ ), and is sandwiched between two  $\text{K}^+(\text{cryptand})$  counter cations (Figure 6a).<sup>[18]</sup> This is the first structural analysis of the tetraarene-fused COT dianion (see below).<sup>[9]</sup> The planar structure of **1a** $^{2-}$  is stabilized by contribution of the  $10\pi$  aromaticity of the COT dianion. The low level of steric hindrance between the adjacent thiazole units is also believed to contribute to its complete planarization. Short intramolecular N—S contacts (2.72 Å) are observed between the adjacent nitrogen and sulfur atoms (Figure 6b); this distance is significantly shorter

than the sum of the van der Waals radii (3.35 Å).<sup>[24]</sup> The bonding orbital interaction is observed between the adjacent nitrogen and sulfur atoms and involves the occupied molecular orbitals HOMO-9 and HOMO-10, although a bond critical point (BCP) was not found by the atoms-in-molecules (AIM) calculations (see the Supporting Information).<sup>[25]</sup>

The aromaticity of **1a** $^{2-}$  was assessed in terms of both magnetic and structural criteria. The large negative NICS(0) and NICS(1) values<sup>[21]</sup> (−14.8 and −12.5 ppm, respectively) of the central COT moiety in **1a** $^{2-}$  supports the high aromaticity;  $^1\text{H}$  NMR analysis is not an appropriate experimental diagnostic in this case because no protons are located near the central COT moiety. More direct evidence of the high aromaticity was obtained in the form of the observed small C—C bond length alternation in the central eight-membered ring. The bond lengths of the planar COT unit are significantly deformed from those of the noncharged species **1a**. Upon reduction, the C—C bonds connecting the two adjacent thiazole rings are shortened from 1.47 to 1.41 and 1.42 Å, while the thiazole-fused C—C bonds are elongated from 1.38 to 1.43 and 1.44 Å (Figure 6b). The planarized COT unit in **1a** $^{2-}$  has a substantially higher HOMA (harmonic oscillator model of aromaticity)<sup>[26]</sup> value (+0.63) than **1a** (+0.17). This result clearly demonstrates the high aromaticity of the  $10\pi$  COT dianion.

In summary, we have synthesized head-to-tail cyclic thiazole tetramers, which represent a  $\pi$ -expanded COT with a remarkable molecular flexibility. The fusion of thiazole rings to the cyclooctatetraene (COT) structure in such a way that they are linked in a head-to-tail fashion results in 1) a shallow saddle-shaped structure with columnar stacking in crystals, 2) a low tub-to-tub inversion barrier of  $\Delta G^\ddagger = 6.8 \text{ kcal mol}^{-1}$  at 298 K, and 3) a compound that can be reduced to the planar aromatic dianion. Most strikingly, the low tub-to-tub inversion barrier of  $6.8 \text{ kcal mol}^{-1}$  is only slightly higher than the umbrella inversion barrier of  $\text{NH}_3$  ( $5.5 \text{ kcal mol}^{-1}$ ).<sup>[27]</sup> In light of the fact that the inversion of amines can occur even in the crystalline state,<sup>[28]</sup> we are interested in applications that may be based on such molecular flexibility of **1** in the solid-state. Future investigations will explore dynamic molecular functions using this new COT core skeleton.

Received: February 15, 2012  
Published online: May 3, 2012

**Keywords:** aromaticity · cyclooctatetraenes · molecular dynamics · thiazoles · redox chemistry

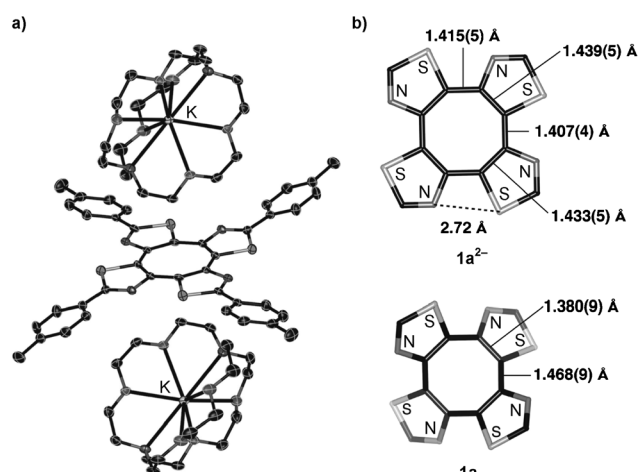


**Figure 6.** a) X-ray crystal structure of dianion **1a** $^{2-} \cdot 2[\text{K}(\text{cryptand})]^+$ . Thermal ellipsoids are shown at 50% probability and hydrogen atoms and solvent molecules (THF) are omitted for clarity; b) the geometries of the central COT moiety of the dianion **1a** $^{2-} \cdot 2[\text{K}(\text{cryptand})]^+$  (upper) and of **1a** (lower).

- [1] a) L. T. Scott, M. M. Hashemi, M. S. Bratcher, *J. Am. Chem. Soc.* **1992**, *114*, 1920; b) T. J. Seiders, K. K. Baldridge, G. H. Grube, J. S. Siegel, *J. Am. Chem. Soc.* **2001**, *123*, 517; c) A. Sygula, *Eur. J. Org. Chem.* **2011**, 1611.  
[2] a) H. Sakurai, T. Daiko, T. Hirao, *Science* **2003**, *301*, 1878; b) T. Amaya, H. Sakane, T. Muneishi, T. Hirao, *Chem. Commun.* **2008**, 765; c) U. D. Priyakumar, G. N. Sastry, *J. Phys. Chem. A* **2001**, *105*, 4488.  
[3] a) W. H. Laarhoven, W. J. C. Prinsen, *Top. Curr. Chem.* **1984**, *125*, 63; b) K. P. Meurer, F. Vögtle, *Top. Curr. Chem.* **1985**, *127*, 1;



- c) R. H. Janke, G. Haufe, E.-U. Würthwein, J. H. Borkent, *J. Am. Chem. Soc.* **1996**, *118*, 6031.
- [4] P. Osswald, F. Würthner, *Chem. Eur. J.* **2007**, *13*, 7395.
- [5] a) M. Stępień, N. Sprutta, L. Latos-Grażyński, *Angew. Chem.* **2011**, *123*, 4376; *Angew. Chem. Int. Ed.* **2011**, *50*, 4288; b) S. Saito, A. Osuka, *Angew. Chem.* **2011**, *123*, 4432; *Angew. Chem. Int. Ed.* **2011**, *50*, 4342.
- [6] T. Nishinaga, T. Ohmae, M. Iyoda, *Symmetry* **2010**, *2*, 76.
- [7] a) R. Breslow, *Acc. Chem. Res.* **1973**, *6*, 393; b) F. W. B. Einstein, A. C. Willis, W. R. Cullen, B. L. Soulen, *J. Chem. Soc. Chem. Commun.* **1981**, 526; c) L. A. Paquette, T.-Z. Wang, C. E. Cottrell, *J. Am. Chem. Soc.* **1987**, *109*, 3730; d) A. Matsuura, K. Komatsu, *J. Am. Chem. Soc.* **2001**, *123*, 1768; e) F.-G. Klärner, *Angew. Chem.* **2001**, *113*, 4099; *Angew. Chem. Int. Ed.* **2001**, *40*, 3977; f) T. M. Krygowski, E. Pindelska, M. K. Cyrański, G. Häfelfinger, *Chem. Phys. Lett.* **2002**, *359*, 158; g) C. S. Wannere, D. Moran, N. L. Allinger, B. A. Hess, Jr., L. J. Schaad, P. v. R. Schleyer, *Org. Lett.* **2003**, *5*, 2983; h) R. W. A. Havenith, P. W. Fowler, L. W. Jenneskens, *Org. Lett.* **2006**, *8*, 1255; i) T. Nishinaga, T. Uto, R. Inoue, A. Matsuura, N. Treitel, M. Rabinovitz, K. Komatsu, *Chem. Eur. J.* **2008**, *14*, 2067.
- [8] a) F. A. L. Anet, *J. Am. Chem. Soc.* **1962**, *84*, 671; b) J. F. M. Oth, *Pure Appl. Chem.* **1971**, *25*, 573; c) Z. Luz, S. Meiboom, *J. Chem. Phys.* **1973**, *59*, 1077; d) C. Trindle, T. Wolfskill, *J. Org. Chem.* **1991**, *56*, 5426; e) J. L. Andrés, O. Castaño, A. Morreale, R. Palmeiro, R. Gomperts, *J. Chem. Phys.* **1998**, *108*, 203.
- [9] a) T. J. Katz, *J. Am. Chem. Soc.* **1960**, *82*, 3785; b) S. Z. Goldberg, K. N. Raymond, C. A. Harmon, D. H. Templeton, *J. Am. Chem. Soc.* **1974**, *96*, 1348; c) A. Sygula, F. R. Fronczek, P. W. Rabideau, *J. Organomet. Chem.* **1996**, *526*, 389.
- [10] a) G. A. Olah, J. S. Staral, L. A. Paquette, *J. Am. Chem. Soc.* **1976**, *98*, 1267; b) G. A. Olah, J. S. Staral, G. Liang, L. A. Paquette, W. P. Melega, M. J. Carmody, *J. Am. Chem. Soc.* **1977**, *99*, 3349; c) T. Nishinaga, K. Komatsu, N. Sugita, *J. Chem. Soc. Chem. Commun.* **1994**, 2319.
- [11] W. Heinz, H.-J. Räder, K. Müllen, *Tetrahedron Lett.* **1989**, *30*, 159.
- [12] a) M. J. Marsella, R. J. Reid, *Macromolecules* **1999**, *32*, 5982; b) M. J. Marsella, R. J. Reid, S. Estassi, L.-S. Wang, *J. Am. Chem. Soc.* **2002**, *124*, 12507.
- [13] A. Sygula, F. R. Fronczek, R. Sygula, P. W. Rabideau, M. M. Olmstead, *J. Am. Chem. Soc.* **2007**, *129*, 3842.
- [14] T. Nishiuchi, Y. Kuwatani, T. Nishinaga, M. Iyoda, *Chem. Eur. J.* **2009**, *15*, 6838.
- [15] T. Ohmae, T. Nishinaga, M. Wu, M. Iyoda, *J. Am. Chem. Soc.* **2010**, *132*, 1066.
- [16] For a selection of reports on the direct arylation of the thiazole ring at the 4- or 5-positions, see: a) A. Yokooji, T. Okazawa, T. Satoh, M. Miura, M. Nomura, *Tetrahedron* **2003**, *59*, 5685; b) B. Liégault, D. Lapointe, L. Caron, A. Vlassova, K. Fagnou, *J. Org. Chem.* **2009**, *74*, 1826; c) B. Liégault, I. Petrov, S. I. Gorelsky, K. Fagnou, *J. Org. Chem.* **2010**, *75*, 1047.
- [17] The DFT calculations were performed by Gaussian09 program (see the Supporting Information).
- [18] CCDC 865419 (**1a**), 865420 (**2a**), 865421 (**1a**<sup>2-</sup>-2 [K-(cryptand)]<sup>+</sup>), and 865418 (**5a**) contain the supplementary crystallographic data for this paper. These data can be obtained free of charge from The Cambridge Crystallographic Data Centre via [www.ccdc.cam.ac.uk/data\\_request/cif](http://www.ccdc.cam.ac.uk/data_request/cif).
- [19] S. M. H. Kabir, M. Miura, S. Sasaki, G. Harada, Y. Kuwatani, M. Yoshida, M. Iyoda, *Heterocycles* **2000**, *52*, 761.
- [20] N. Z. Huang, T. C. W. Mak, *J. Chem. Soc. Chem. Commun.* **1982**, 543. See also the Supporting Information.
- [21] a) P. v. R. Schleyer, C. Maerker, A. Dransfeld, H. Jiao, N. J. R. v. E. Hommes, *J. Am. Chem. Soc.* **1996**, *118*, 6317; b) P. v. R. Schleyer, M. Manoharan, Z.-X. Wang, B. Kiran, H. Jiao, R. Puchta, N. J. R. v. E. Hommes, *Org. Lett.* **2001**, *3*, 2465.
- [22] E. Kraka, D. Cremer, *Acc. Chem. Res.* **2010**, *43*, 591.
- [23] The difference in the bent angles between the crystal structure (29.4°) and the optimized structure (34.5°) of **1** is presumably due to the effect of the packing force in the columnar stacking.
- [24] a) H. Pang, P. J. Skabara, D. J. Crouch, W. Duffy, M. Heeney, I. McCulloch, S. J. Coles, P. N. Horton, M. B. Hursthouse, *Macromolecules* **2007**, *40*, 6585; b) G. J. McEntee, F. Vilela, P. J. Skabara, T. D. Anthopoulos, J. G. Labram, S. Tierney, R. W. Harrington, W. Clegg, *J. Mater. Chem.* **2011**, *21*, 2091.
- [25] a) "Atoms in Molecules: A Quantum Theory": R. F. W. Bader in *the International Series of Monographs of Chemistry* (Eds.: J. Halpen, M. L. H. Green), Clarendon, Oxford, **1990**; b) R. F. W. Bader, *J. Phys. Chem. A* **1998**, *102*, 7314.
- [26] T. M. Krygowski, M. K. Cyrański, *Chem. Rev.* **2001**, *101*, 1385.
- [27] A. M. Halpern, B. R. Ramachandran, E. D. Glendening, *J. Chem. Educ.* **2007**, *84*, 1067. See also the Supporting Information.
- [28] G. A. Sim, *J. Chem. Soc. Chem. Commun.* **1987**, 1118.